Research Square

Preprints are preliminary reports that have not undergone peer review.
They should not be considered conclusive, used to inform clinical practice,
or referenced by the media as validated information.

Development of a voltage-divider based probe method for sheet resistance measurement of copper foils and thin films

Mehrangiz Kazemi
Babol Noshirvani University of Technology
Hossein Miar-Naimi
Babol Noshirvani University of Technology
Majid Abbasi
Babol Noshirvani University of Technology
Marzieh Abbasi-Firouzjah
abbasimarzieh@gmail.com

Hakim Sabzevari University

Research Article

Keywords: Sheet resistance, Electrical resistivity, Voltage division, Copper thin film, Single-point probe

Posted Date: October 21st, 2026

DOI: https://doi.org/10.21203/rs.3.rs-11225161/v1

License: This work is licensed under a Creative Commons Attribution 4.0 International License.
Read Full License

Additional Declarations: No competing interests reported.

Version of Record: A version of this preprint was published at Journal of Materials Science: Materials in Electronics on November 3rd, 2026. See the published version at https://doi.org/10.1007/s10854-026-18802-8.

Development of a voltage-divider based probe method for sheet resistance measurement of copper foils and thin films

Mehrangiz Kazemi[a], Hossein Miar-Naimi[b], Majid Abbasi[a] , Marzieh Abbasi-Firouzjah[c,d*]

[a] *Faculty of Materials and Industrial Engineering, Babol Noshirvani University of Technology, Mazandaran, Iran.*
[b] *Department of Electrical and Computer Engineering, Babol Noshirvani University of Technology, Mazandaran, Iran. Orcid No.0000-0003-0758-9949.*
[c] *Department of Engineering Sciences, Hakim Sabzevari University, Sabzevar, Iran, Orcid No.0000-0001-7625-3993.*
[d] *Faculty of Chemical and Materials Engineering, Shahrood University of Technology, Shahrood, Iran.*

Abstract

Accurate measurement of sheet resistance is essential for the electrical characterization of thin metallic films and foils, particularly when sample dimensions and thickness approach the limits of conventional probe-based techniques. In this study, a voltage-divider-based probe method was developed for measuring the sheet resistance of copper samples over micrometer- and nanometer-scale thicknesses. The proposed system combines a controlled electrical measurement circuit with a digital data-acquisition unit and was designed to reduce the sensitivity of the measurement to probe spacing and sample geometry under defined dimensional conditions. Copper foils with thicknesses from 20 to 100 μm and thermally evaporated copper films with thicknesses of approximately 32–529 nm were investigated. The sheet resistance and electrical resistivity obtained using the proposed method were compared with measurements performed using a conventional four-point probe. For micrometer-thick copper foils, the two methods produced closely comparable resistivity values, demonstrating the reproducibility of the proposed approach. At the nanometer scale, the proposed method remained capable of measuring samples thinner than 100 nm, for which the four-point probe measurements were not obtained under the experimental conditions used in this study. The measured resistivity increased with decreasing film thickness, consistent with enhanced electron scattering associated with size-dependent transport. The results demonstrate that the proposed voltage-divider-based method can provide a simple and reproducible approach for sheet-resistance characterization of small copper foils and thin films, while its applicability to ultrathin and non-uniform samples should be considered within the assumptions of the measurement model.

Keywords: Sheet resistance, Electrical resistivity, Voltage division, Copper thin film, Single-point probe

* Corresponding author

E-mail address: abbasimarzieh@gmail.com

1. Introduction

Thin metallic films and foils are widely used in electronic and optoelectronic technologies, where electrical properties such as sheet resistance and electrical resistivity directly influence device performance, current transport, interconnect reliability, and functional behavior [1-3]. In thin-film systems, the electrical response can differ substantially from that of the corresponding bulk material because the reduction in film thickness changes the relative contribution of surface, interface, grain boundary, and defect-related scattering mechanisms [4-6]. Consequently, reliable measurement of sheet resistance is an important part of the electrical characterization of thin films and thin metallic layers [1].

For a homogeneous film of thickness (t), sheet resistance (R_S) is related to electrical resistivity (ρ) through ($R_S = \rho$ /t) [8]. Although this relationship is straightforward, accurate determination of R_S and ρ can become challenging when the film thickness, lateral dimensions, or electrical uniformity of the sample are reduced. In particular, the measured electrical response may be affected by probe geometry, probe spacing, sample boundaries, contact resistance, surface morphology, and thickness non-uniformity. [9-12] These factors become increasingly important for nanoscale metallic films, where the film thickness can approach characteristic electron transport length scales [4,5,13].

The linear four-point probe is one of the most widely used techniques for sheet-resistance and resistivity measurements of conductive thin films. In this configuration, two outer probes supply the current while two inner probes measure the resulting voltage, minimizing the influence of contact resistance on the measured voltage. [7,14] The method provides reliable measurements when the sample dimensions, thickness, probe spacing, and probe positions satisfy the assumptions associated with the analytical model [9-11]. However, finite sample dimensions and probe placement may require geometric and thickness correction factors. Alternative configurations, including square four-point probes and the Van der Pauw method, can extend the applicability to different sample geometries, but they also impose specific requirements on probe arrangement, sample dimensions, contact configuration, or sample uniformity. Recent thin-film studies continue to employ four-point probe and Van der Pauw configurations as standard approaches for electrical characterization. [10-12,15]

Despite their established reliability, conventional probe techniques can become less convenient when the available sample area is small, the sample geometry is non-standard, or measurements are required over a wide thickness range. For ultrathin metallic films, additional complications arise from thickness non-uniformity and size-dependent electron scattering. [10-12] Therefore, a measurement approach that combines a simple electrical configuration with controlled data acquisition and reduced sensitivity to probe arrangement could be useful as a complementary technique for thin-film characterization.

The thickness dependence of electrical resistivity is also of fundamental importance in metallic thin films. When the film thickness becomes comparable to characteristic electron mean-free-path or grain dimensions, surface and grain boundary scattering can make significant contributions to electron transport. The resulting increase in resistivity with decreasing thickness has been described using classical size-effect models and has been experimentally observed in Cu thin-film systems. Recent studies of metallic thin films have likewise demonstrated the importance of film thickness in determining electrical resistivity and sheet resistance. These effects make copper a suitable model material for evaluating a measurement method over both micrometer and nanometer thickness regimes. [16-18]

Despite the availability of established contact-based and contactless techniques, there remains practical interest in simple measurement configurations that can provide reproducible sheet-resistance data while reducing the dependence of the measurement on probe arrangement and sample geometry [11, 12, 19]. In particular, a measurement approach that combines a simple electrical circuit, controlled data acquisition, and a theoretically defined relationship between probe spacing and sample dimensions could provide a useful complementary method for conductive foils and thin films.

In the present work, a voltage-divider-based probe measurement system is developed for the determination of sheet resistance and electrical resistivity of copper foils and thin films. The measurement system combines a controlled voltage-divider circuit, signal amplification, and digital data acquisition to obtain the electrical response of the sample. Copper foils with micrometer-scale thicknesses and thermally evaporated copper films with nanometer-scale thicknesses are investigated. The proposed method is evaluated by comparison with a conventional four-point probe measurement for samples for which the reference technique provides measurable results. In addition, the influence of sample thickness on the measured electrical resistivity is examined to assess the applicability of the proposed approach to nanoscale copper films. The theoretical basis of the proposed measurement configuration is established using the electrical potential distribution in a conductive sheet, and the resulting dimensional conditions for its application are experimentally evaluated. The study therefore focuses not only on the development of a measurement device, but also on the validation, operating conditions, and practical limitations of the proposed sheet-resistance measurement approach.

2. Experimental details

2.1. Sample preaparation and characterization

To investigate the performance of the proposed measurement method over different dimensional scales, copper samples with micrometer- and nanometer-scale thicknesses were prepared. Copper foils with different thicknesses were produced by cold rolling. A rolling mill with a roller diameter of 80 mm was

operated at a speed of 30 rpm using a lubricant during the rolling process. The initial copper foil had a thickness of 100 μm and was progressively reduced to nominal thicknesses of 85, 70, 65, 60, 55, 50, 40, 30, and 20 μm. The thickness of the rolled foils was determined using three independent methods: a precision thickness gauge (PTG100), a micrometer with an accuracy of 1 μm, and an optical microscope (MDS) operated at a magnification of 400×. Measurements at different positions of the foils were performed to evaluate the thickness uniformity.

Copper thin films with nominal thicknesses of approximately 32, 53, 90, 213, and 529 nm were deposited on glass substrates using vacuum-assisted thermal evaporation. Prior to deposition, the glass substrates were ultrasonically cleaned using alcohol and acetone and subsequently dried. During deposition, the vacuum level was maintained at $4*10^{-3}$ Pa. The thickness of the deposited copper films was determined from cross-sectional field-emission scanning electron microscopy (FE-SEM; Sigma 300-HV). Cross-sectional images obtained from different positions were analyzed using ImageJ, and the average film thickness was determined from the measured values. The uncertainty or variation in film thickness was subsequently considered in the analysis of the electrical properties.

The electrical resistance of the copper foils and thin films was characterized using both a conventional four-point probe and the proposed voltage-divider-based method. For the reference measurements, a commercial Jandel four-point probe device with a probe spacing of 1–3 mm was employed. The probes were positioned approximately at the center of the copper samples. The two outer probes were used to supply the measurement current (I), while the two inner probes were used to measure the voltage drop (V) across the sample. This four-terminal configuration separates the current and voltage contacts and consequently reduces the contribution of contact and lead resistances to the measured voltage. The four-point probe technique and the influence of probe geometry on resistivity measurements have been extensively discussed in the literature [2,20].

Because the measured resistance in a four-point configuration depends on the sample geometry, probe spacing, thickness, and probe arrangement, appropriate geometric correction factors may be required when the sample dimensions are not sufficiently large compared with the probe spacing. Recent analyses have also demonstrated that correction factors can depend on the geometry and non-ideal dimensions of the sample [3, 21]. Therefore, in the present work, the four-point-probe measurements were used as a reference measurement under the same sample and experimental conditions rather than assuming that the four-point-probe result is completely independent of sample geometry.

For each sample, twenty measurements were performed at different locations within the central region of the sample, and the arithmetic mean was used as the reported value.

2.2. Design of the sheet resistance measurement circuit

A dedicated measurement system was designed and constructed to determine the electrical resistance of conductive samples using a voltage-divider configuration. The flowchart of the design procedure and the manufacturing steps of the measurement device are shown in Fig. 1. The electrical circuit was first simulated using Proteus software, and the control algorithm was subsequently implemented using the Arduino development environment.

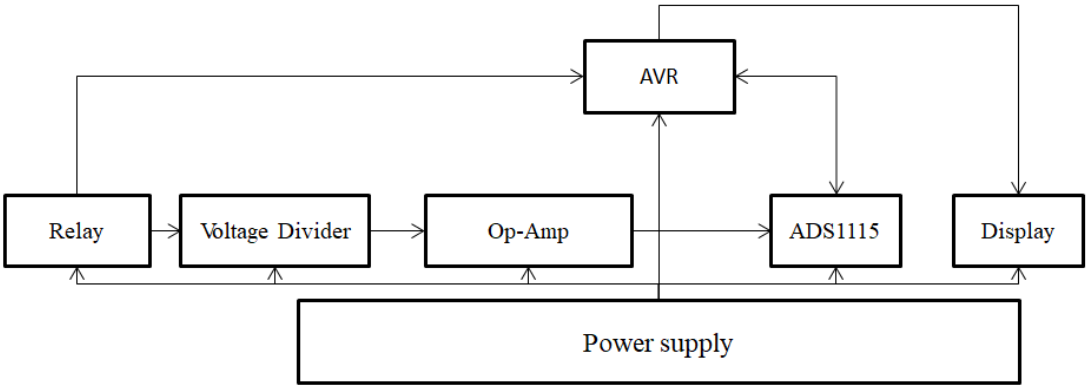


Fig. 1. Flowchart of the design process and manufacturing steps of a single-point probe device for sheet resistance measuring.

The proposed measurement circuit is based on a series voltage-divider configuration. The unknown resistance of the sample, (R_s), is connected in series with a reference resistance, (R_1), across the input voltage (V_i). The voltage developed across the sample is measured as (V_o). Therefore, for the circuit shown in Fig. 2, the output voltage is given by

$$V_o = V_i \times \frac{R_s}{R_1 + R_s} \tag{1}$$

Accordingly, the resistance of the sample (R_s) can be obtained from the measured voltage [22]. The voltage-divider relationship is a standard electrical measurement principle. Thus, the accuracy of the calculated resistance depends on the accuracy and stability of the reference resistance (R_1), the input voltage (V_i), and the measured output voltage (V_o).

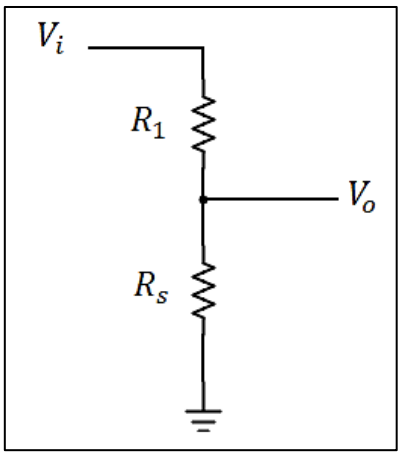


Fig. 2. Voltage divider circuit for sheet resistance measurement.

In the proposed system, the effective value of (R_1) was determined independently before the measurements by short-circuiting the two electrical contacts that normally connect to the sample. This procedure provides an experimental estimate of the resistance associated with the electrical measurement path and contacts. The experimentally determined value was subsequently used in the resistance calculations. This calibration procedure was employed to reduce systematic errors associated with the electrical connections between the measurement circuit, probes, and sample.

Because the output voltage of the voltage-divider circuit can be relatively small, an amplification stage was incorporated before analog-to-digital conversion. The amplifier was configured for differential voltage measurement with a sufficiently high input impedance so that the voltage-measurement stage would have a limited effect on the voltage-divider circuit. The amplified voltage signal was subsequently digitized for numerical processing. The use of an appropriate electrical characterization and measurement configuration is particularly important when the measured resistance is affected by parasitic and contact resistances. [23]

The electrical resistivity of a conductor is temperature dependent. Therefore, a relay was incorporated into the measurement circuit to control the duration for which current was applied to the sample. A 5-V, five-terminal relay was used to connect and disconnect the measurement circuit during the measurement sequence. By reducing the duration of current flow through the sample, the relay operation was intended to minimize possible Joule-heating effects during resistance measurement. This procedure is particularly relevant for thin conductive samples because temperature changes can influence their measured electrical resistance.

The measured electrical resistance was subsequently related to the sheet resistance through the theoretical model described in Section 2.4. The electrical resistivity was then calculated from the sheet resistance and the independently measured sample thickness.

2.3. Signal acquisition and control system

The measurement system was controlled using an Arduino UNO board based on the ATmega328P microcontroller. The Arduino platform was used for relay control, acquisition sequencing, communication with the display module, and data-processing operations. The hardware specifications of the Arduino UNO and its ATmega328P controller are documented by the manufacturer [24].

To improve the resolution of the voltage acquisition, an ADS1115 analog-to-digital converter (ADC) was incorporated into the measurement system instead of relying solely on the internal ADC of the Arduino UNO. The ADS1115 is a 16-bit, four-channel delta-sigma ADC equipped with a programmable gain amplifier (PGA) and an I²C digital communication interface. [25] The use of the external ADC provides a higher nominal voltage resolution than the 10-bit ADC integrated into the Arduino UNO and is therefore particularly useful for measuring the relatively small voltage variations generated by the voltage-divider circuit.

The amplified output voltage from the measurement circuit was applied to the ADS1115 input and converted into a digital signal. The ADS1115 communicated with the Arduino UNO through the I²C interface, and the acquired voltage data were transferred to the microcontroller for subsequent resistance calculation. The measured output voltage (V_o), together with the input voltage (V_i) and the experimentally determined reference resistance (R_1), was then used in the voltage-divider relation to calculate the sample resistance.

The measurement sequence was programmed so that relay switching, voltage acquisition, and resistance calculation were performed in a controlled and repeatable order. The use of an external high-resolution ADC and a programmable acquisition sequence allowed the voltage measurement and subsequent resistance calculation to be performed under identical conditions for repeated measurements.

2.4. Calculation of resistance between two points on an infinite conductive plane of conductor

As described, the proposed measurement method determines the electrical resistance from the voltage response of the sample. To establish the relationship between the measured voltage, current, sample conductivity, and the dimensions of the measurement region, the electric potential distribution between

two hypothetical points on an extended conducting plane was considered. The analysis is based on the Laplace equation ($\nabla^2 V = 0$) for the electric potential in a homogeneous conducting medium. The same type of potential-field formulation is commonly used in electrical characterization and resistivity analysis. [26]

For a two-dimensional conducting plane in Cartesian coordinates, the Laplace equation is written as

$$\frac{\partial^2 V}{\partial x^2} + \frac{\partial^2 V}{\partial y^2} = 0 \tag{2}$$

The differential equation can be solved by the method of separation of variables, assuming that $V = V_x V_y$, i.e. the spatial dependence of V in the x and y directions can be represented by independent functions. Substitution of this expression into Eq. (2) gives

$$V_x'' V_y + V_x V_y'' = 0 \tag{3}$$

This relationship holds under the following condition:

$$\frac{V_x''}{V_x} = \frac{-V_y''}{V_y} = \alpha^2 \tag{4}$$

where α is a constant. To solve the above equation, the homogeneous equation $V_x'' / V_x = \alpha^2$ is first solved; it has real roots. Then the homogeneous equation $V_y'' \mp \alpha^2 V_y = 0$ is solved; the roots of this equation are complex.

$$V_x = A_1 e^{\alpha x} + A_2 e^{-\alpha x}$$

$$\mathrm{V_y = A_3 \cos \alpha y + A_4 \sin \alpha y} \tag{5}$$

The general solution of the equation is obtained as

$$\mathrm{V = \left(A_1 e^{\alpha x} + A_2 e^{-\alpha x} \right)\left(A_3 \cos \alpha y + A_4 \sin \alpha y \right)} \tag{6}$$

Time and space-dependent boundary conditions are used to determine the constants (Fig. 3). The potential function for $\mathrm{x > 0}$ is abotained as

$$\begin{cases} \mathrm{V\left(x = +\infty, y\right) = 0 \rightarrow\ A_1 = 0} \\ V\left(x, y = 0\right) = 0 \rightarrow\ A_3 = 0 \\ V\left(x, y\right) = A_2 A_4 e^{-\alpha x} \sin \alpha y \\ V\left(x, y\right) = A e^{-\alpha x} \sin \alpha y \end{cases} \tag{7}$$

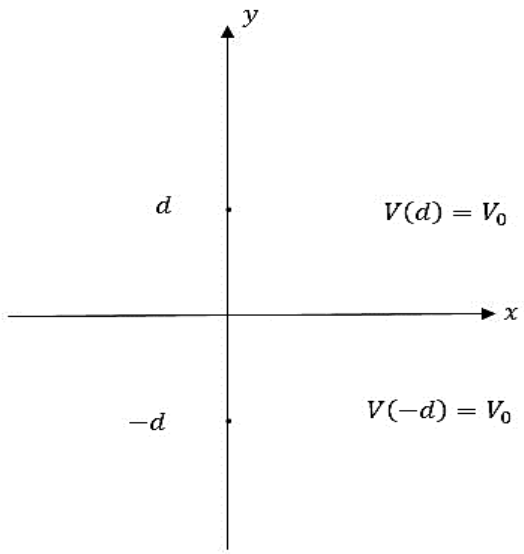


Fig. 3. Two hypothetical points on the infinite plane of the conductor to calculate the resistance.

Where, $A_2A_4 = A$. The following relations are also obtained for the boundary conditions x=0 and y=±d:

$$\begin{cases} V\left(x=0, y=d\right)=V_0 \\ A\sin\alpha d = V_0 \\ V\left(x=0, y=-d\right)=-V_0 \\ A\sin\left(-\alpha d\right)=-V_0 \end{cases} \tag{8}$$

where V_0 is the maximum electrical potential and $-V_0$ is the minimum electrical potential, with $\alpha d = \frac{\pi}{2}$, and $A = V_0$. Finally the solution of the equation is obtained as

$$V\left(x,y\right) = V_0 e^{-\frac{\pi x}{2d}} \sin\frac{\pi}{2d} y \tag{12}$$

Having obtained the function V, the electric field is calculated from $E = -\nabla V$:

$$E = -\nabla V = \left(\frac{-\partial V}{\partial x}, \frac{-\partial V}{\partial y}\right) = \left(\frac{-\partial V}{\partial x} a_x + \frac{-\partial V}{\partial y} a_y\right) \tag{9}$$

$$E = \left(\frac{V_0\pi}{2d} e^{-\frac{\pi x}{2d}} \sin\frac{\pi y}{2d}, \frac{-V_0\pi}{2d} e^{-\frac{\pi x}{2d}} \cos\frac{\pi y}{2d}\right) \tag{10}$$

$$E = \frac{V_0\pi}{2d} e^{-\frac{\pi x}{2d}} \left(\sin\frac{\pi y}{2d} a_x - \cos\frac{\pi y}{2d} a_y\right) \tag{11}$$

When an electric field E is applied to a material, it produces an electric current. The electric current density per unit area is given by J = σE, where σ is the conductivity.

$$\mathrm{J}=\sigma\mathrm{E}=\sigma\frac{\mathrm{V}_0\pi}{2\mathrm{d}}\mathrm{e}^{-\frac{\pi\mathrm{x}}{2\mathrm{d}}}\left(\sin\frac{\pi\mathrm{y}}{2\mathrm{d}}\mathrm{a}_\mathrm{x}-\cos\frac{\pi\mathrm{y}}{2\mathrm{d}}\mathrm{a}_\mathrm{y}\right) \tag{12}$$

Thus, the current density along the x-axis is obtained as

$$J\left(y=0\right)=\sigma\frac{V_0\pi}{2d}e^{-\frac{\pi x}{2d}}\left(-a_y\right) \tag{13}$$

Finally, the current in the plane x > 0 for a conductor of thickness Δ is

$$I=\int_0^\infty J\left(y=0\right)ds=\int_0^\infty Jdx\,\Delta\left(-ay\right) \tag{14}$$

$$\mathrm{I}=\int_0^\infty\sigma\frac{\mathrm{V}_0\pi}{2\mathrm{d}}\mathrm{e}^{-\frac{\pi\mathrm{x}}{2\mathrm{d}}}\mathrm{dx}\Delta=\sigma\frac{\mathrm{V}_0\pi}{2\mathrm{d}}\left(\frac{2\mathrm{d}}{-\pi}\right)\mathrm{e}^{-\frac{\pi\mathrm{x}}{2\mathrm{d}}}\Big|_0^\infty\Delta \tag{15}$$

$$\mathrm{I}=\sigma\mathrm{V}_0\Delta \tag{16}$$

According to the symmetry of the conducting plane, the same current flows through the corresponding region on the (x<0) side. Therefore, the total current is

$$I_t=2I=2\sigma V_0\Delta \tag{17}$$

The resistance between the two hypothetical points can consequently be expressed as

$$\mathrm{R}=\frac{1}{\sigma\Delta} \tag{18}$$

As can be seen, the value of R is independent of D, where D denotes the dimensions of the conductor plate. This follows from the assumption, made in solving the problem, that the plane is infinitely large, with the value of infinity placed at the boundary D/2 (Fig. 4). For this assumption to be valid, the following relations must hold

$$\mathrm{e}^{-\frac{\pi}{2\mathrm{d}}\cdot\frac{\mathrm{D}}{2}}\approx\mathrm{e}^{-\infty}=0 \tag{19}$$

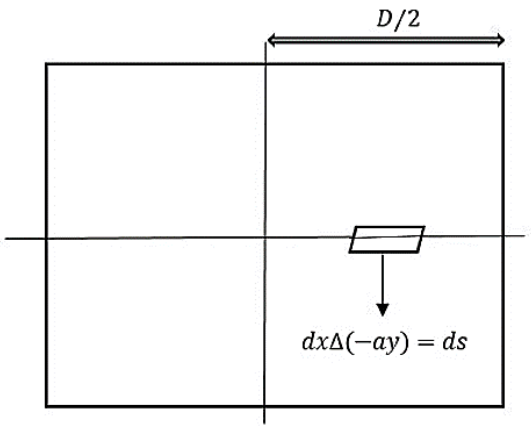


Fig. 4. The area element (ds) to calculate the cross-sectional area of electric current.

A practical condition for this approximation is

$$\begin{cases} \dfrac{\pi}{2\mathrm{d}} \cdot \dfrac{\mathrm{D}}{2} \geq 4 \\ \dfrac{\mathrm{D}}{\mathrm{d}} \geq \dfrac{16}{\pi} \\ \dfrac{\mathrm{D}}{\mathrm{d}} \geq 5 \end{cases} \tag{20}$$

Accordingly, the distance between the measurement points should be less than approximately one-fifth of the characteristic dimension of the sheet. Here, (D) represents the relevant lateral dimension of the finite sample and (d) represents the distance parameter used in the theoretical model. Therefore, the proposed method does not require an assumption of an infinitely large sample in the actual experiment; rather, the infinite-plane solution is used when the dimensional condition in Eq. (20) is satisfied.

The proposed approach is not intrinsically limited to copper. For another conductive or semiconductive material, the conductivity in Eq. (12) changes according to the material, while the geometrical derivation remains applicable provided that the assumptions of homogeneous conductivity and the adopted boundary conditions are reasonably satisfied.

For the experimental measurements, the resistance obtained from the voltage-divider circuit was therefore combined with the geometrical relation derived above to determine the sheet resistance. The electrical resistivity was subsequently calculated using the independently measured thickness of the sample. Repeated measurements were performed under identical conditions to evaluate the repeatability of the proposed method. For the copper foils, 20 repeated measurements were obtained for each selected thickness. The results were compared with the corresponding four-point-probe measurements. The

influence of sample thickness and the distance between measurement points was then evaluated using the experimental results and the dimensional condition given by Eq. (20).

3. Results and discuttion

3.1. Measurement of copper sheet resistance in micrometric dimensions

Figure 5(a) presents the sheet resistance of the rolled copper foils with thicknesses of 100, 85, 70, 65, 55, 50, 40, 30, and 20 μm, as measured using both the proposed single-point probe method and the conventional four-point probe method. For each sample, twenty measurements performed at different positions. The maximum measurement variation was obtained $5\times10^{-5}\Omega$, which is sufficiently small that the corresponding error bars are not clearly visible in the graph. This relatively small variation indicates good repeatability of the proposed measurement procedure under the conditions used in this study.

The electrical resistivity calculated from the measured sheet resistance and independently measured sample thickness is presented in Fig. 5(b). For the proposed single-point probe method and the four-point probe method, the electrical resistivity was calculated using the corresponding sheet-resistance relations given in the theoretical model and the sample thickness. The two methods show generally consistent trends over the investigated micrometer-scale thickness range. The differences between the two methods are relatively small compared with the measured values, indicating that the proposed voltage-divider-based approach can provide comparable sheet-resistance and resistivity measurements for the rolled copper foils under the experimental conditions used in this work.

The four-point probe is a widely used reference technique for determining sheet resistance. however, the measured value can be affected by probe spacing, sample dimensions, thickness, probe position, and the associated geometrical correction factors [3, 15, 27]. These effects become particularly relevant when the dimensions of the sample are not sufficiently large compared with the probe spacing. In the present work, the proposed method was derived using an extended-plane approximation, and Eq. (20) provides a dimensional condition under which the effect of the finite sample boundary can be considered sufficiently small. Therefore, within the dimensional range satisfying Eq. (20), the measured resistance of the proposed method is expected to show reduced sensitivity to the distance between the measurement points.

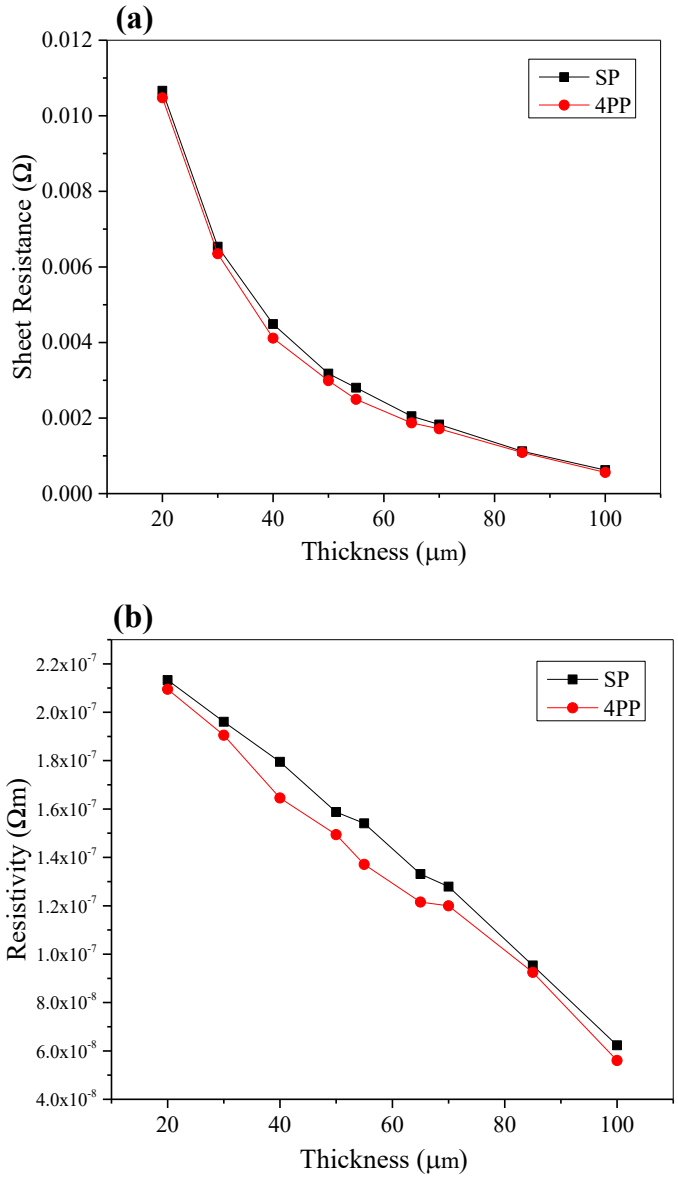


Fig. 5. (a) Sheet resistance and (b) electrical resistivity as a function of thickness measured by single-probe and four-point probe methodes.

The experimental results support this theoretical consideration. When the distance between the measurement points was maintained within the dimensional condition obtained from Eq. (20), no substantial systematic variation in the measured sheet resistance was observed. This behavior should not be interpreted as complete independence from probe spacing; rather, it indicates that the effect of probe spacing is sufficiently small within the geometrical range investigated in this study. This distinction is important because both the proposed method and conventional four-point measurements are ultimately affected by the finite dimensions and electrical uniformity of the sample.

The sheet resistance and electrical resistivity both increase as the thickness of the copper foil decreases, as shown in Fig. 5. This trend is consistent with the relation between sheet resistance, resistivity, and thickness, $R_s=\rho/t$.

For the rolled copper foils, however, the change in resistivity cannot be attributed solely to the geometrical reduction in thickness. Cold rolling modifies the microstructure of the material, including grain structure, dislocation density, residual stress, and defect population. These microstructural changes can influence electron scattering and consequently the measured resistivity [28]. Previous investigations of rolled and thin copper structures have similarly reported a relationship between thickness, microstructure, grain structure, and electrical transport properties. [10,28]

The measured results therefore indicate that the proposed method is capable of following the expected thickness-dependent electrical response of copper foils in the micrometer range. The agreement between the two measurement techniques also provides an experimental validation of the proposed voltage-divider-based measurement approach for samples satisfying the geometrical assumptions of the theoretical model.

To further investigate whether the measured sheet resistance can be used to estimate the thickness of an unknown copper foil, a calibration relationship between sheet resistance and thickness was established using the samples with known thicknesses, as shown in Fig. 6. The experimental data were fitted using the regression relation reported in Fig. 6.

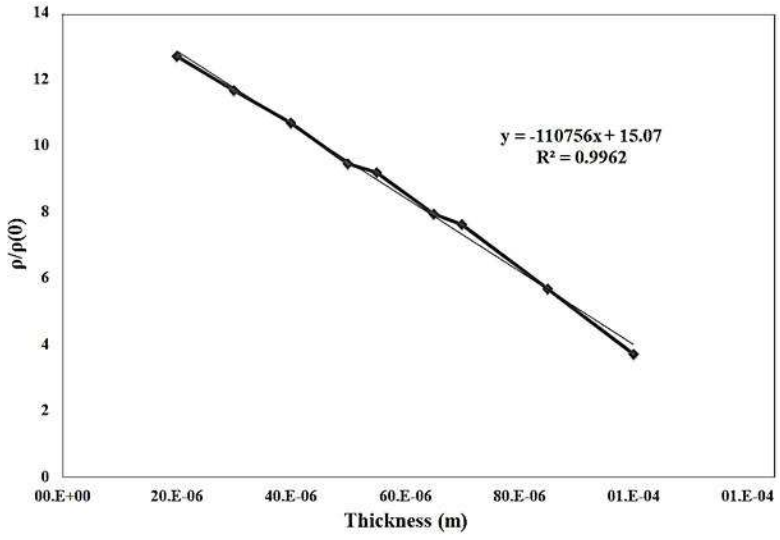


Fig 6. Variation of ρ/ρ_0 as a function of thickness.

The coefficient of determination obtained from the regression was 99.62%, indicating a strong correlation between the measured sheet resistance and the thickness of the investigated copper foils. It should be noted that this calibration relationship is specific to the material, preparation procedure, and measurement conditions used in this study and should not be regarded as a universal thickness–resistance relation for copper.

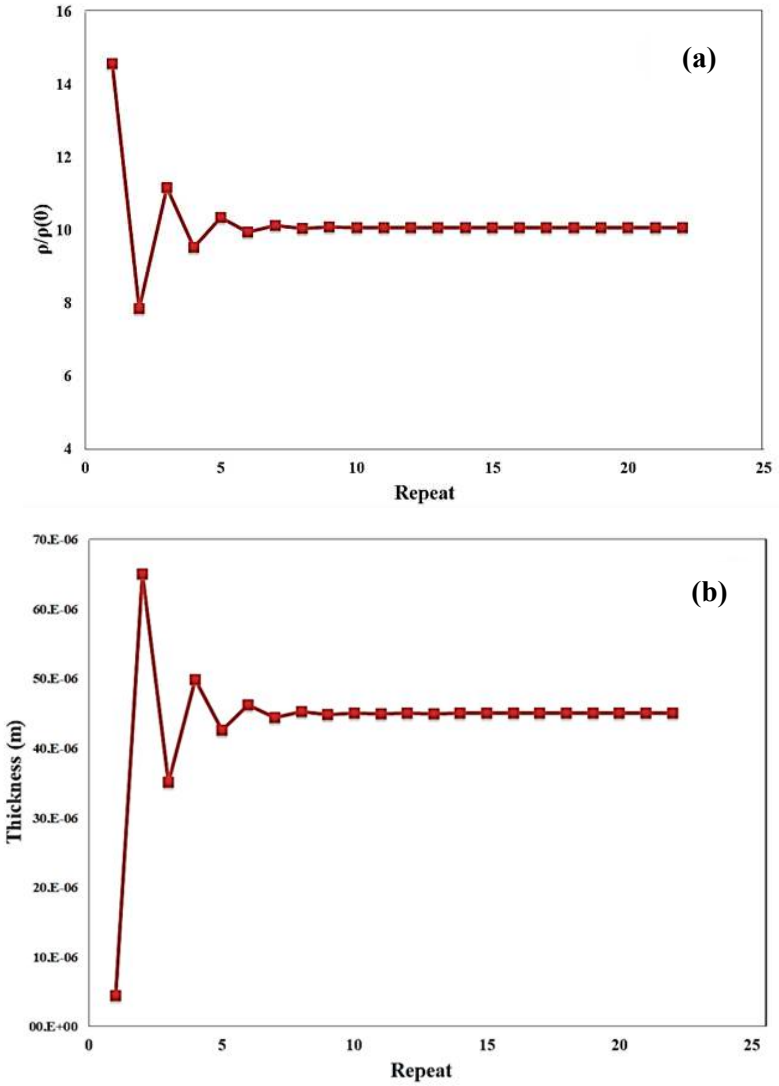


Fig 7. Calculation of unknown thickness with measured surface resistance $R_s = 0.002358$ (a) Iteration ρ/ρ_0, (b) Iteration of thickness.

The calibration curve was subsequently used to estimate the thickness of two copper samples for which the thickness was treated as unknown during the electrical measurement. The thickness values obtained from the proposed method were approximately 45 and 60 μm, respectively. These values were subsequently compared with independent measurements obtained using the PTG100 precision thickness

gauge (see Figs 7 and 8). The agreement between the electrical calibration and the independent thickness measurement demonstrates the potential of the proposed method for indirect thickness estimation when the material resistivity and sample preparation conditions are sufficiently controlled. Similar approaches based on sheet-resistance measurements have previously been investigated for thickness determination of conductive thin films [5].

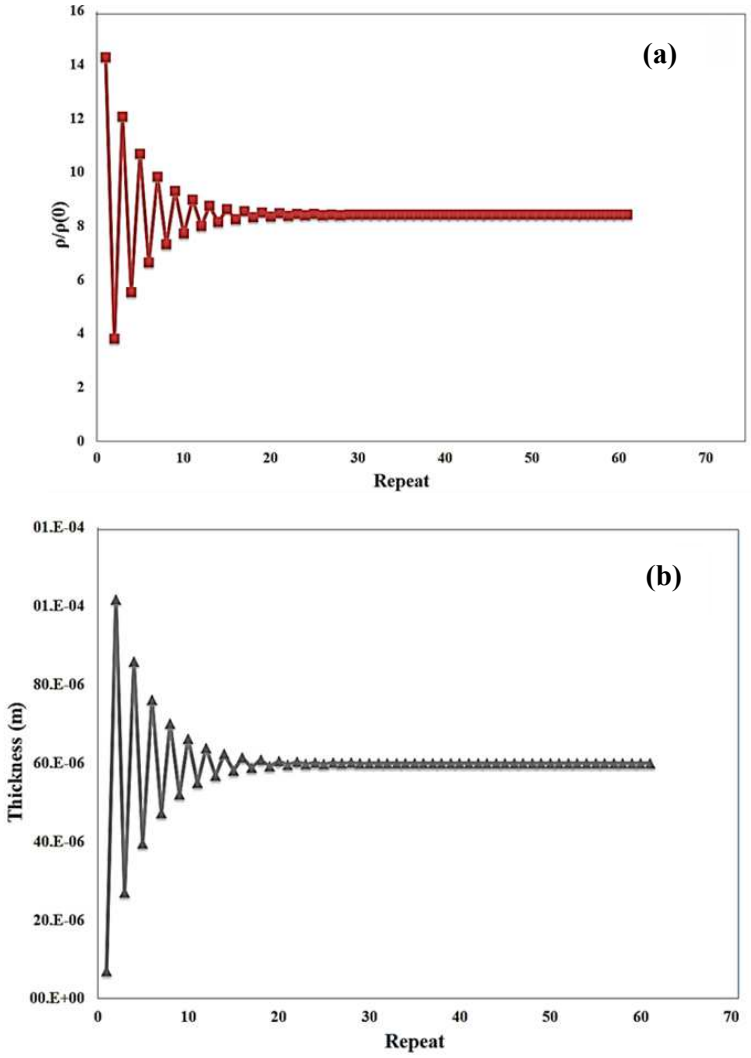


Fig 8. Calculation of unknown thickness with measured surface resistance $R_s = 0.003765$. (a) Iteration ρ/ρ_0, (b) Iteration of thickness.

3.2. Measurement of copper sheet resistance in nanometer dimensions

To evaluate the performance of the proposed measurement method at the nanoscale, five thermally evaporated copper films with nominal thicknesses of approximately 32, 53, 90, 213, and 529 nm were investigated. The measured thicknesses, together with their experimental variations, were approximately

32 ± 4%, 53 ± 4%, 90 ± 5%, 213 ± 6%, and 529 ± 7%, respectively. Figures 9(a)-9(d) show the cross-sectional FE-SEM image of copper deposited thin films with different thicknesses. The sheet resistance and electrical resistivity obtained using the proposed single-point probe and four-point probe methods are summarized in Table 1. The values obtained using the proposed method represent the average of 20 repeated measurements. The relatively small variations observed between repeated measurements indicate good repeatability of the proposed measurement system for the investigated samples.

For the 90, 213, and nm films, both measurement methods produced measurable values. The difference between the two methods was approximately 5%, 20%, and 28%, respectively. For the 32 and 53 nm films, however, the four-point-probe system used in this study did not provide measurable sheet-resistance values under the experimental conditions employed. This observation should be interpreted as a limitation of the measurement configuration used in the present study rather than as an intrinsic lower-thickness limit of the four-point-probe technique. Four-point measurements can be affected by contact quality, probe geometry, sample continuity, sheet resistance magnitude, and the electrical properties of ultrathin films [1,2].

The measured sheet resistance obtained using the proposed method increases substantially with decreasing film thickness. A corresponding increase in electrical resistivity is also observed. This trend is consistent with the well-established size effect in metallic thin films. When the film thickness becomes comparable to characteristic electron transport length scales, electron scattering at surfaces and grain boundaries contributes increasingly to the total resistivity [3,29]. For copper, the electron mean free path is of the order of several tens of nanometers; a value of approximately 39 nm has been reported at room temperature depending on the definition and calculation approach used. [30,31] Recent experimental studies of Cu films with thicknesses ranging from tens of nanometers to several micrometers have also demonstrated increased electron scattering as the film thickness decreases. [10,11]

The thickness dependence observed in the present work is therefore physically reasonable. For the thickest films, the film thickness is substantially larger than the characteristic electron mean free path, and the relative contribution of surface scattering to the total resistance is reduced. As the thickness decreases toward the nanoscale, the probability of electron interaction with film surfaces and grain boundaries increases, resulting in higher electrical resistivity. This behavior has been reported experimentally for Cu thin films over a wide range of thicknesses. [10,11,30]

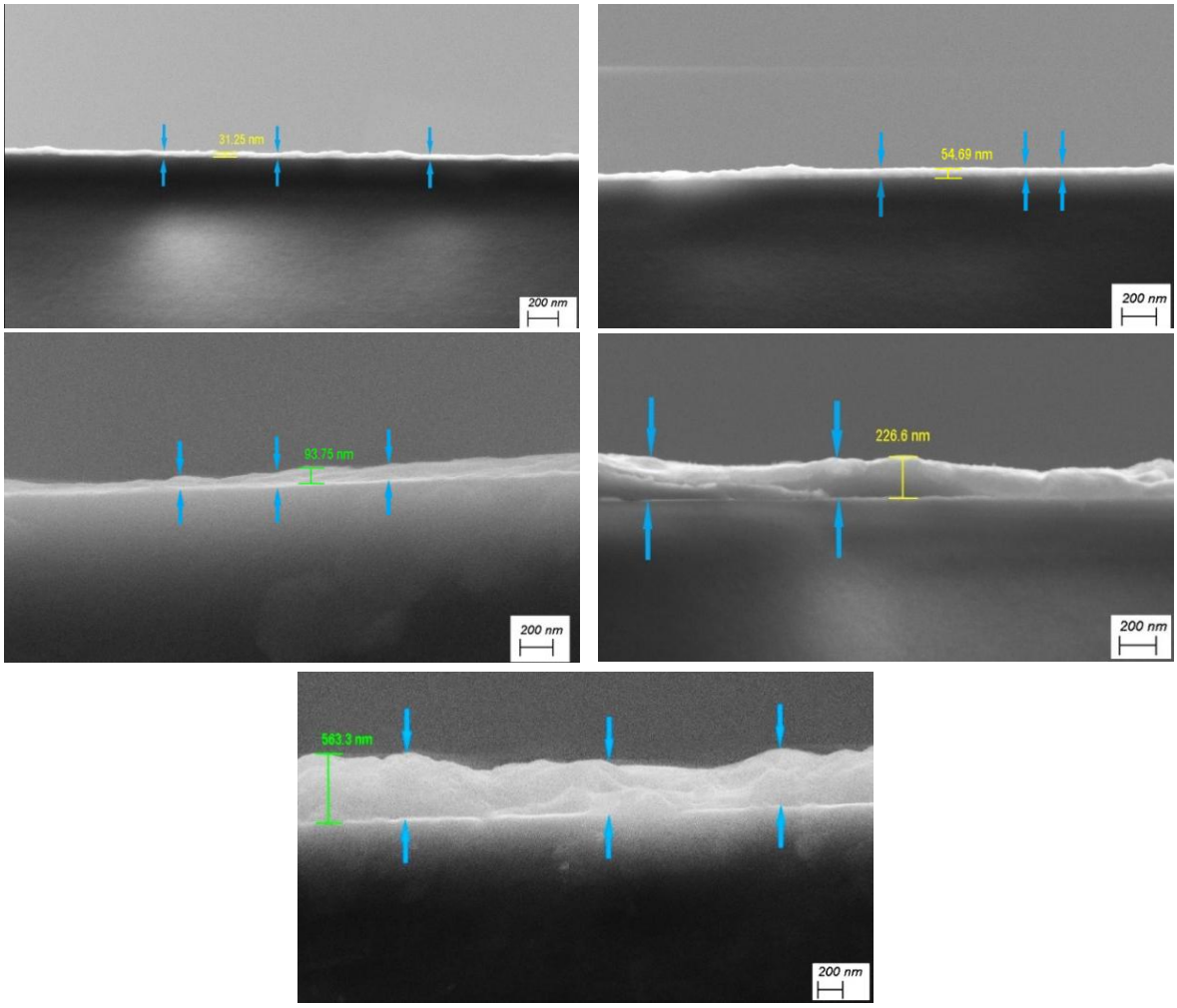


Fig 9. Cross-sectional FESEM image of the cross-sectional surface of pure copper coating with the thickness of about (a) 34 nm, (b) 53 nm, (c) 90 nm, (d) 213 nm, and (e) 529 nm.

Table 1. Sheet resistance and electrical resistivity of nanometer samples measured by single-point probe and four-point probe methods.

Thickness (nm)	Sheet resistance (Ω)			Electrical resistivity (Ωm)	
	Four-probe	Single-probe	Difference percentage	Four-probe	Single-probe
32±4%	—	3047.24 ± 0.01%	—	—	9.75×10^{-5}
53±4%	—	1226.9 ± 0.03%	—	—	6.50×10^{-5}
90±5%	173.67	182.22 ± 0.2%	5%	1.56×10^{-5}	1.63×10^{-5}
213±6%	5.56	6.93 ± 0.9%	20%	1.18×10^{-6}	1.47×10^{-6}
529±7%	1.98	2.75 ± 0.5%	28%	1.05×10^{-6}	1.45×10^{-6}

Surface morphology can further influence the electrical transport of ultrathin Cu films. Timalsina et al. demonstrated that nanoscale surface roughness contributes to the residual resistivity of ultrathin epitaxial copper films [13], while more recent work has also shown that surface morphology and film continuity can strongly influence the electrical resistance of thermally evaporated ultrathin Cu films [31]. Therefore, the relatively nonuniform surface observed in the thicker evaporated films may contribute to the difference between the two measurement methods. However, because the present study does not include an independent quantitative measurement of surface roughness, the contribution of roughness cannot be separated from the effects of thickness variation, probe contact, and measurement geometry.

Figure 10 also shows the variation of surface resistance and specific resistance as a function of thickness for nanometer samples related to single-point probe method. According to both diagrams, with the decrease in thickness, an increase in surface resistance and specific resistance has occurred.

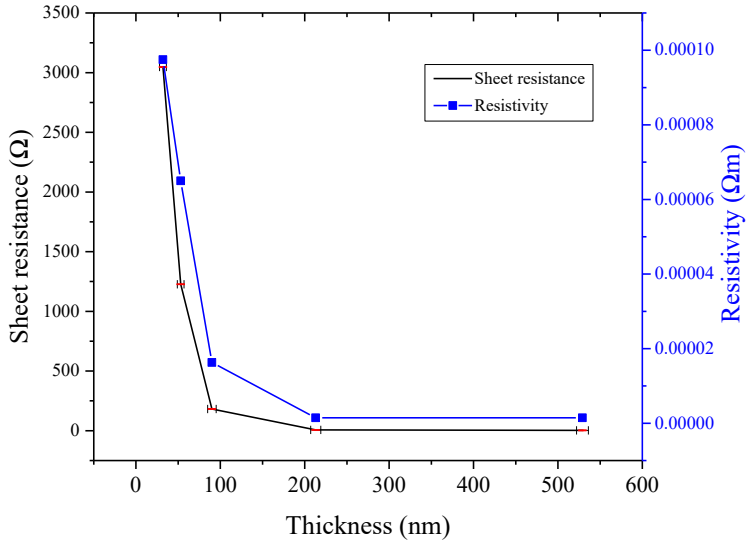


Fig. 10. Sheet resistance and electrical resistivity as a function of thickness measured by single-point probe method in nanometer thicknesses.

Interestingly, the 213 and 529 nm samples exhibited relatively high repeatability in the proposed measurement, with the reported measurement variation remaining below approximately 1%. Although the surfaces of these films were not perfectly uniform, their thicknesses were considerably larger than the electron mean free path. Consequently, small-scale surface nonuniformities are expected to have a smaller relative influence on the overall electrical transport than in ultrathin films. At the same time, the differences between the proposed and four-point-probe measurements for these two samples were larger than those observed for the 90 nm film. Rather than assigning these differences exclusively to measurement error in the four-point probe, they should be considered as the combined result of probe

geometry, sample uniformity, contact conditions, thickness uncertainty, and the different measurement configurations.

For the films with thicknesses below 100 nm, the proposed method provided measurable and repeatable values, whereas the four-point-probe system used in this study did not provide measurable results for the 32 and 53 nm films. The increased sensitivity of electrical resistance to thickness and surface condition in this thickness regime is consistent with previous investigations of ultrathin Cu films. The results therefore demonstrate the practical capability of the proposed method to extend the electrical characterization performed in this work to film thicknesses for which the reference four-point measurement was not successful under the same experimental conditions.

The difference between the proposed and four-point methods for the measurable nanometer-scale samples was below 30%. Although this difference is larger than that observed for the micrometer-scale copper foils, it should be considered in relation to the substantially greater sensitivity of nanoscale electrical transport to thickness uncertainty, surface morphology, grain structure, and contact conditions. Recent studies have similarly shown that electrical transport in Cu films becomes increasingly sensitive to surface and grain boundary scattering as the characteristic dimensions approach the nanoscale [3,11,17,31].

The role of grain boundaries in the measured resistivity can be understood in terms of electron scattering at internal interfaces. Experimental investigations have shown that grain boundary scattering can make a substantial contribution to the resistivity of nanometric metallic structures [17]. For Cu conductors, the contribution of grain size, impurity scattering, geometry, and electron–phonon interactions has also been investigated, demonstrating that several scattering mechanisms can contribute simultaneously to the measured resistivity [18]. Therefore, the increase in resistivity observed in the present nanometer-scale Cu films should be regarded as a combined size-dependent transport effect rather than being attributed to a single scattering mechanism.

In addition to grain boundary scattering, surface roughness and impurities can affect the resistivity of nanoscale copper. [13,18] The presence of impurities or deviations from ideal stoichiometric purity can introduce additional electron-scattering centers, while surface roughness modifies the probability of electron–surface scattering. The contribution of these mechanisms is particularly important when the film thickness approaches the characteristic transport length scale [13,30]. Because the present study does not include independent quantitative characterization of impurity concentration, grain size, or surface roughness, these mechanisms are discussed as possible contributors rather than as independently quantified sources of the measured resistance.

Overall, the nanometer-scale measurements show that the proposed voltage-divider-based method reproduces the expected increase in sheet resistance and electrical resistivity with decreasing Cu film thickness. The agreement with the available four-point-probe measurements, together with the repeatability of the proposed method, supports its use as a complementary electrical measurement approach for thin conductive films. Nevertheless, the larger differences observed at the nanoscale emphasize that the accuracy of the method is increasingly affected by film uniformity, thickness uncertainty, surface morphology, grain structure, and contact conditions.

4. Conclusion

A voltage-divider-based measurement method was developed and experimentally evaluated for determining the sheet resistance of copper foils and thermally evaporated copper thin films. The proposed method determines the electrical resistance from the measured voltage response of a series voltage-divider circuit and subsequently obtains the sheet resistance and electrical resistivity using the theoretical and geometrical relations developed in this study.

Copper foils with thicknesses in the range of 20–100 μm and thermally evaporated copper films with thicknesses of approximately 32–529 nm were investigated. For the micrometer-scale copper foils, the proposed method produced sheet-resistance and electrical-resistivity values that were generally consistent with those obtained using a conventional four-point probe. The 20 repeated measurements performed for each foil thickness also demonstrated good measurement repeatability.

The theoretical analysis shows that the proposed method can be treated using an infinite-plane approximation when the distance between the measurement points satisfies the dimensional condition derived in Eq. (20). Under this condition, the influence of the finite sample boundary and the measurement-point separation is sufficiently reduced. Therefore, the proposed method should not be considered completely independent of probe spacing; rather, its sensitivity to probe spacing is reduced within the specified geometrical range.

The calibration relationship obtained from the micrometer-scale copper foils showed a coefficient of determination of 99.62%. The calibration curve was successfully used to estimate the thickness of two copper samples, yielding values of approximately 45 and 60 μm, which were subsequently compared with measurements obtained using an independent precision thickness gauge. This result indicates that the proposed electrical measurement can also be used for indirect thickness estimation when a suitable calibration relationship is established for a given material and measurement condition.

For the nanometer-scale copper films, the measured sheet resistance and electrical resistivity increased with decreasing film thickness. This behavior is consistent with the size-dependent electrical transport of metallic thin films and can be associated with the increasing contribution of surface, grain boundary, and other defect-related scattering mechanisms as the film thickness approaches characteristic electron transport length scales. For the 90, 213, and 529 nm films, the proposed and four-point-probe methods gave comparable results, with differences of approximately 5%, 20%, and 28%, respectively. For the 32 and 53 nm films, the four-point-probe system used in this study did not provide measurable values under the experimental conditions, whereas the proposed method provided repeatable measurements.

The proposed method therefore provides a simple and experimentally reproducible approach for sheet-resistance characterization of conductive samples over micrometer- and nanometer-scale thickness ranges. Its principal advantages are the relatively simple electrical configuration, controlled voltage acquisition, reduced sensitivity to probe spacing within the theoretical dimensional condition, and applicability to samples for which conventional four-point measurements may be difficult under specific experimental conditions. At the same time, the method relies on assumptions concerning sample homogeneity, thickness, conductivity, and boundary conditions. Consequently, its accuracy can decrease for highly nonuniform, discontinuous, or microstructured ultrathin films.

The present results demonstrate the feasibility of the voltage-divider-based approach as a complementary sheet-resistance measurement method rather than as a universal replacement for established four-point-probe techniques. Further improvement of the method should include a quantitative uncertainty analysis, systematic investigation of contact resistance and surface morphology, and validation using additional conductive materials and sample geometries.

References

1. Kariyapperuma, D., Constant, S., Ramsdale, C., Hao, L., “Sheet Resistance Measurements of Conductive Thin Films: A Comparison of Techniques,” *Electronics* 10 (2021) 960. https://doi.org/10.3390/electronics10080960.
2. Miccoli, I., Edler, F., Pfnür, H., Tegenkamp, C., “The 100th anniversary of the four-point probe technique: the role of probe geometries in isotropic and anisotropic systems,” *Journal of Physics: Condensed Matter* 27 (2015) 223201. https://doi.org/10.1088/0953-8984/27/22/223201.
3. Yilmaz, S., “The geometric resistivity correction factor for several geometrical samples,” *Journal of Semiconductors* 36 (2015) 082001. https://doi.org/10.1088/1674-4926/36/8/082001.
4. Cultrera, A., Serazio, D., Fabricius, N., Callegaro, L., “New IEC standards for the measurement of sheet resistance on large-area graphene using the van der Pauw and the in-line four-point probe methods,” *Measurement* 236 (2024) 114980. https://doi.org/10.1016/j.measurement.2024.114980.
5. Kang, J.-H., Lee, S.-H., Ruh, H., Yu, K.-M., “Development of a thickness meter for conductive thin films using four-point probe method,” *Journal of Electrical Engineering & Technology* 16 (2021) 2265–2273. https://doi.org/10.1007/s42835-021-00725-5.

6. Li, J.C., Wang, Y., Ba, D.C., “Characterization of semiconductor surface conductivity by using microscopic four-point probe technique,” *Physics Procedia* 32 (2012) 347–355.

7. Deen, M.J., Pascal, F., “Electrical characterization of semiconductor materials and devices,” *Journal of Materials Science: Materials in Electronics* 17 (2006) 549–575.

8. Polyanin, A.D., Manzhirov, A.V., *Handbook of Integral Equations*, CRC Press, 2008.

9. Akhbarifar, S. et al., *Four-point probe geometric correction factor for isotropic cylindrical samples with non-equal probe distances*, *Measurement* 184, 109703 (2021).

10. Roa, S., Sirena, M., “Size effects on the optimization of the mechanical resistance and the electrical conductivity of Cu thin films,” *Materials Today Communications* 28 (2021) 102572. https://doi.org/10.1016/j.mtcomm.2021.102572.

11. Islam, M.R. et al., *Evaluating size effects on the thermal conductivity and electron-phonon scattering rates of copper thin films for experimental validation of Matthiessen’s rule*, *Nature Communications* 15, 9167 (2024).

12. Hu, C., Zhang, Y., Chen, Z., Zhang, Q., Zhu, J., Hu, S., Ke, Y., “Size effect of resistivity due to surface roughness scattering in alternative interconnect metals: Cu, Co, Ru, and Mo,” *Physical Review B* 107 (2023) 195422. https://doi.org/10.1103/PhysRevB.107.195422.

13. Timalsina, Y.P., Horning, A., Spivey, R.F., Lewis, K.M., Kuan, T.-S., Wang, G.-C., Lu, T.-M., “Effects of nanoscale surface roughness on the resistivity of ultrathin epitaxial copper films,” *Nanotechnology* 26 (2015) 075704. https://doi.org/10.1088/0957-4484/26/7/075704.

14. Balcazar, Luz M., and María de la Luz Olvera Amador. "IGZO thin films deposited by ultrasonic spray pyrolysis: effect of Zn precursor milling and In and Ga concentration." Journal of Materials Science: Materials in Electronics 35.12 (2024): 829.

15. Cultrera, A., Serazio, D., Fabricius, N., Callegaro, L., *New IEC standards for the measurement of sheet resistance on large-area graphene using the van der Pauw and the in-line four-point probe methods*, *Measurement* 236, 114980 (2024).

16. *Temperature-Dependent Sheet Resistance and Surface Characterization of Thin Copper Films Bonded to FR4 Composite under Mechanical Vibrations*, *Applied Sciences* 13, 7941 (2023).

17. Henriquez, R., Cancino, S., Espinosa, A., Flores, M., Hoffmann, T., Kremer, G., Lisoni, J.G., Moraga, L., Morales, R., Oyarzun, S., et al., “Electron grain boundary scattering and the resistivity of nanometric metallic structures,” *Physical Review B* 82 (2010) 113409. https://doi.org/10.1103/PhysRevB.82.113409.

18. Plombon, J.J., Andideh, E., Dubin, V.M., Maiz, J., “Influence of phonon, geometry, impurity, and grain size on copper line resistivity,” *Applied Physics Letters* 89 (2006) 113124. https://doi.org/10.1063/1.2355435.

19. Huang, R., Robl, W., Ceric, H., Detzel, T., Dehm, G., “Stress, sheet resistance, and microstructure evolution of electroplated Cu films during self-annealing,” *IEEE Transactions on Device and Materials Reliability* 10 (2010) 47–54.

20. ASTM International, *ASTM F390, Standard Test Method for Sheet Resistance of Thin Metallic Films with a Collinear Four-Probe Array*.

21. Thorsteinsson, S., Wang, F., Petersen, D.H., et al., “Accurate microfour-point probe sheet resistance measurements on small samples,” *Review of Scientific Instruments*, 80 (2009) 053902. DOI: 10.1063/1.3125050.

22. G. Woan, The Cambridge handbook of physics formulas, Cambridge University Press, 2000.

23. J.H. Moore, C.C. Davis, M.A. Coplan, Building scientific apparatus, Cambridge University Press2009.]

24. Arduino. “Arduino UNO Rev3.” Arduino Documentation, Arduino S.r.l.

25. Texas Instruments. “ADS111x Ultra-Small, Low-Power, I²C-Compatible, 860-SPS, 16-Bit ADCs with Internal Reference, Oscillator, and Programmable Comparator.” ADS1115 Datasheet, Texas Instruments.

26. Deen, M. Jamal, and Fabien Pascal. "Electrical characterization of semiconductor materials and devices." *Journal of Materials Science: Materials in Electronics* 17.8 (2006): 549-575.

27. Zolfaghar Tehrani, S., Lim, W.L., Lee, L., "Correction factors for films resistivity measurement," *Measurement* 45 (2012) 219–225. https://doi.org/10.1016/j.measurement.2011.11.019.

28. Song, M., Liu, X., Liu, L., "Size Effect on Mechanical Properties and Texture of Pure Copper Foil by Cold Rolling," *Materials* 10 (2017) 538. https://doi.org/10.3390/ma10050538

29. Mayadas, A.F., Shatzkes, M., "Electrical-resistivity model for polycrystalline films: The case of arbitrary reflection at external surfaces," *Physical Review B* 1 (1970) 1382–1389. https://doi.org/10.1103/PhysRevB.1.1382

30. Gall, D., "Electron mean free path in elemental metals," *Journal of Applied Physics* 119 (2016) 085101. https://doi.org/10.1063/1.4942216.

31. Gray, G., Marín, F., del Campo, V., González-Fuentes, C., Correa-Puerta, J., Flores, M., Segura, R., Häberle, P., Henríquez, R., "Effect of thiol adsorption on the electrical resistance of copper ultrathin films," *Applied Surface Science* 673 (2024) 160912. https://doi.org/10.1016/j.apsusc.2024.160912.

Statements & Declarations

Funding

The authors declare that no funds, grants, or other support were received during the preparation of this manuscript.

Competing Interests

The authors have no relevant financial or non-financial interests to disclose.

Author contributions

Mehrangiz Kazemi: *Validation, Formal analysis, Investigation, Writing - Original Draft.*
Hossein Miar-Naimi: *Conceptualization, Validation, Methodology, Review & Editing.*
Majid Abbasi: *Conceptualization, Methodology, Supervision, Project administration, Resources.*
Marzieh Abbasi-Firouzjah: *Validation, Investigation, Writing-Original Draft, Review & Editing.*